Available online at www.sciencedirect.com
SCIENCE DIRECT®
Catalysis Today 89 (2004) 479–493
CATALYSIS TODAY
www.elsevier.com/locate/cattod

Design of new catalysts for ecological high-quality transportation fuels by combinatorial computational chemistry and tight-binding quantum chemical molecular dynamics approaches

Momoji Kubo [a], Tsuguo Kubota [a], Changho Jung [a], Minako Ando [a], Satoshi Sakahara [a], Kenji Yajima [a], Kotaro Seki [a], Rodion Belosludov [a], Akira Endou [a], Seiichi Takami [a], Akira Miyamoto [a,b,*]

[a] *Department of Applied Chemistry, Graduate School of Engineering, Tohoku University, Aoba-yama 07, Sendai 980-8579, Japan*
[b] *New Industry Creation Hatchery Center, Tohoku University, Aoba-yama 10, Sendai 980-8579, Japan*

Received 18 August 2003; received in revised form 19 January 2004; accepted 8 March 2004

Abstract

Recently, we introduced a concept of combinatorial chemistry to computational chemistry and proposed a new method called "combinatorial computational chemistry", which enables us to perform a theoretical high-throughput screening of catalysts. In the present paper, we reviewed our recent application of our combinatorial computational chemistry approach to the design of new catalysts for high-quality transportation fuels. By using our combinatorial computational chemistry techniques, we succeeded to predict new catalysts for methanol synthesis and Fischer–Tropsch synthesis. Moreover, we have succeeded in the development of chemical reaction dynamics simulator based on our original tight-binding quantum chemical molecular dynamics method. This program realizes more than 5000 times acceleration compared to the regular first-principles molecular dynamics method. Electronic- and atomic-level information on the catalytic reaction dynamics at reaction temperatures significantly contributes the catalyst design and development. Hence, we also summarized our recent applications of the above quantum chemical molecular dynamics method to the clarification of the methanol synthesis dynamics in this review.

Keywords: Ecological high-quality transportation fuels; Combinatorial computational chemistry; High-throughput screening; Tight-binding quantum chemical molecular dynamics

1. Introduction

Recently, the technologies for the production of high-quality transportation fuels from non-petroleum hydrocarbon resources have attracted considerable attention by scientists and chemical companies, according to the recent environmental demands and decrease in the fossil energy reserves. The development of highly active and highly selective catalysts for methanol synthesis and Fischer–Tropsch synthesis is strongly demanded in order to advance the industry of the high-quality transportation fuels. Although huge amounts of knowledge on the catalysts for the methanol synthesis and Fischer–Tropsch synthesis have been accumulated, the development of more active and more selective catalysts is strongly demanded. It is well noticed that atomistic information on the catalytic reaction mechanism and catalytic activity is essential for further advance and development of those catalysts. Especially, computational chemistry approach is expected to play an important role to clarify the mechanism of catalytic reactions and to design new catalysts on electronic and atomic levels.

The impacts of computational chemistry on the catalyst research and development are rapidly increased. Especially, the recent advance of first-principles calculation method is significant and it can calculate the formation energy of molecules and solids with high accuracy. Hence, computational chemistry is expected to work as a highly efficient design tool of catalysts. However, the present

* Corresponding author. Tel.: +81-22-217-7233; fax: +81-22-217-7235.
E-mail address: miyamoto@aki.che.tohoku.ac.jp (A. Miyamoto).

0920-5861/$ – see front matter © 2004 Elsevier B.V. All rights reserved.
doi:10.1016/j.cattod.2004.03.055

computational chemistry is mainly employed to clarify the atomistic mechanism of the well-known catalytic reactions and to obtain the electronic information on the catalysts of which property and reactivity are well known experimentally. For example, recently there are a lot of precise calculations for the Cu/ZnO methanol synthesis catalysts to clarify the chemical reaction mechanism of methanol synthesis processes [1–9]. However, there are very few theoretical calculations for the search and design of new catalysts over the Cu/ZnO catalysts for the methanol synthesis. We strongly insisted that such traditional computational chemistry cannot contribute to the design and development of new catalysts.

Hence, recently we paid attention to "combinatorial chemistry" technique, which has been developed as an experimental high-throughput screening method. It enables us to synthesize hundreds of samples all at once and examine their properties. Originally, combinatorial chemistry has been developed mainly in the synthesis of organic compounds and recently introduced into inorganic [10–14] and catalyst [15–17] fields. We noticed that combinatorial chemistry approach could be combined with computational chemistry and it would be a powerful tool to perform a theoretical high-throughput screening. Therefore, more recently we introduced a concept of combinatorial chemistry to computational chemistry and proposed a new method "combinatorial computational chemistry" [18–22]. In this concept, computational chemistry is employed to perform a high-throughput screening of the catalysts including active metals, supports, and additives. We also succeeded to develop new computer cluster system and software to realize our combinatorial computational chemistry by using grid-computing technology. The activity, selectivity, and functionality of a lot of catalysts are calculated systematically, and the best catalyst can be efficiently and speedily proposed by using our new method. This new methodology is expected to predict completely new catalysts with high activity, high selectivity, and high resistance to poisons, theoretically. Moreover, our approach can propose new guidance to predict highly active and highly selective catalysts. We have already applied our combinatorial computational chemistry approach to the design of the zeolite catalysts for the deNO_x reaction and proposed that IrZSM-5 has the highest tolerance to water poisoning [18–20]. After our proposal, the validity of IrZSM-5 was confirmed experimentally. Moreover, we confirmed the effectiveness and applicability of our combinatorial computational chemistry not only for catalysts but also for electronics materials, batteries, ceramics and so on [21,22].

We have also applied our combinatorial computational chemistry approach to the design and high-throughput screening of catalysts for ecological high-quality transportation fuels and succeeded to predict new catalysts for methanol synthesis and Fischer–Tropsch synthesis [23–28]. Hence, in the present paper we reviewed our recent application of combinatorial computational chemistry techniques to the high-throughput screening of new catalysts for methanol synthesis and Fischer–Tropsch synthesis and introduced our success of new catalysts design.

On the other hand, electronic- and atomic-level information on the catalytic reaction dynamics at reaction temperatures significantly contributes the catalyst design and development. However, the first-principles method can only calculate the static electronic states at 0.0 K, and hence it cannot elucidate the catalytic reaction dynamics at reaction temperatures. Therefore, we have recently succeeded in the development of a chemical reaction dynamics simulator based on our original tight-binding quantum chemical molecular dynamics method [29–36]. This program realizes more than 5000 times acceleration compared to the regular first-principles molecular dynamics method. It means that our new program is very effective for the investigations of the catalytic reaction dynamics on huge catalyst models including active metals, supports, and additives, compared to the regular first-principles molecular dynamics simulations. We have already applied it to various catalyst systems including Cu/ZnO methanol synthesis catalysts and have succeeded to clarify the atomistic catalytic reaction dynamics at reaction temperatures. Hence, in this review we also introduced and summarized our recent applications of the chemical reaction dynamics simulator based on our tight-binding quantum chemical molecular dynamics method to the clarification of the methanol synthesis reaction dynamics.

2. Methods

2.1. Combinatorial computational chemistry based on first-principles calculation

Combinatorial computational chemistry based on the density functional theory (DFT) calculations [37,38] is performed by using DMol [39,40] program in Section 3 and ADF [41–44] program in Sections 4 and 5. In the DMol program, linear combination of numerical atomic orbitals is used in the Kohn–Sham formulation. The structure optimization and energy calculations are carried out by local density approximation (LDA) with Vosko–Wilk–Nusair (VWN) functional [45]. Double numerical basis sets with polarization functions (DNP) are employed. In the ADF program, linear combination of Slater-type atomic orbitals is used. The structure optimization is carried out by local density approximation with VWN functional [45] and the energy of the optimized structure is calculated by generalized gradient approximation (GGA) with Becke 88 [46] and Perdew-Wang 91 functionals [47]. Triple-ζ basis sets with polarization functions (TZP) are employed. The computer graphics pictures of catalyst models and calculation results are produced by the Cerius^2 program developed by MSI Inc.

2.2. Development of new software for combinatorial computational chemistry

We employed grid-computing technology to use many computers efficiently for the high-throughput screening of catalysts. Our computer cluster system is composed of one main computer and other many Linux computers. The main computer arranges all the jobs for the high-throughput screening and throws a job to each Linux computer. In order to perform the high-throughput screening efficiently, the main computer checks the CPU state of all the Linux computers and automatically throws new job just after the finish of the job in the Linux computer. Moreover, the main computer has another important role. It automatically collects all the calculation results from the Linux computers and analyzes the results.

Moreover, we developed new software to perform combinatorial computational chemistry in the above computer cluster system. The new software realizes automatic modeling of a large number of catalysts by the continuous replacement of elements in the catalyst model by using main computer. Moreover, it automatically performs the first-principles calculations of the large number of catalyst models by using many Linux computers and grid-computing technology. It also automatically transfers all the calculation results from the Linux computers to the main computer and realizes the automatic analysis of the optimized structure, bond distance, electronic states, electron transfer, bond population, and so on in the main computer. These new software and computer cluster system for combinatorial computational chemistry are very useful to perform a theoretical high-throughput screening of a large number of catalysts and to propose a new high performance catalyst among a large number of candidates.

2.3. Original tight-binding quantum chemical molecular dynamics simulator

Chemical reaction dynamics simulator "Colors" was developed on the basis of our original tight-binding quantum chemical molecular dynamics method. The equations to be solved in this simulator are shown in Eqs. (1) and (2)

$$HC = SC\varepsilon \tag{1}$$

$$C^{\mathrm{T}}SC = I \tag{2}$$

where H is the Hamiltonian matrix, S the overlap matrix, C the eigenvector matrix, ε the eigenvalue matrix, and C^{T} is the transformation matrix of C. The total energy in the system is calculated employing Eqs. (3) and (4)

$$E = \sum_{i=1}^{n}\frac{1}{2}m_i v_i^2 + \sum_{k}^{\mathrm{occ}}\varepsilon_k + \sum_{i=1}^{n}\sum_{j=i+1}^{n}\frac{Z_i Z_j e^2}{R_{ij}} + \sum_{i=1}^{n}\sum_{j=i+1}^{n}E_{ij}^{\mathrm{repul}}(R_{ij}) \tag{3}$$

$$E_{ij}^{\mathrm{repul}}(R_{ij}) = f_0 b_{ij}\exp\left(-\frac{R_{ij}-a_{ij}}{b_{ij}}\right) \tag{4}$$

In these formulas, m_i is the atomic weight, v_i the atomic velocity, e the elementary electric charge, R_{ij} the interatomic distance, and f_0 (=6.9511 × 10^{-11} N) is constant for unit adaptations. The parameters a_{ij} and b_{ij} are related to the size and stiffness of two atoms, respectively. Z_i is the atomic charge obtained by the tight-binding electronic states calculation. Here, Mulliken analysis is employed to evaluate the above atomic charge. The first term refers to the kinetic energy of the atoms, the second term is the summation of the eigenvalues of all the occupied orbitals calculated by the tight-binding electronic states calculation, and the third term represents the Coulomb interaction. The last term corresponds to the short-range exchange repulsion energy.

Many tight-binding approximations were already proposed and applied to various systems. However, the previous tight-binding approximations can calculate only the covalent systems such as silicon and diamond semiconductors, since the long-range Coulomb interaction is neglected [48–51]. On the other hand, our new tight-binding theory considers the long-range Coulomb interactions by the introduction of the third term in Eq. (3). This extension is revolutionary, since it enables us to apply the tight-binding theory to almost all materials including oxides, nitrides, sulfides, metals, and others. Namely, our new theory solved the main problem of the previous tight-binding theory, which is its limited applicability to only the covalent systems. This is a main characteristic of new tight-binding theory developed by us.

The validity of our new tight-binding theory was evaluated by comparing with the density functional theory calculations. We calculated a lot of small cluster models, such as $Si(OH)_4$, $Si_2O_7H_6$, $Si(OCH_3)_4$, H_2O, H_2O_2, and so on by our new tight-binding quantum chemical molecular dynamics method, and quantitatively same atomic charges, energies, and bond distances with density functional theory calculation results were obtained [30,32,33]. Hence, we confirmed the high accuracy and high validity of our new tight-binding quantum chemical molecular dynamics method.

The computer graphics pictures of catalyst models and calculation results are produced by RYUGA program developed in our laboratory [52].

3. Design of new methanol synthesis catalysts [23,24]

3.1. Introduction

Industrially, methanol is synthesized from a mixture of CO and H_2 at temperature of 500–550 K over $Cu/ZnO/Al_2O_3$ catalyst and it has been experimentally pointed out that Cu^+ cation is an active site for the methanol synthesis [53,54]. The formation mechanism of the methanol from CO and H_2 has not been well established

by experiments. However, some mechanisms are strongly supported by experimental data. Here, we introduce two different mechanisms of the methanol synthesis process.

- Mechanism (a)

$$M + CO \rightarrow MCO \quad (5)$$

$$MCO + H_2 \rightarrow MCHOH \quad (6)$$

$$MCHOH + \tfrac{1}{2}H_2 \rightarrow MCH_2OH \quad (7)$$

$$MCH_2OH + \tfrac{1}{2}H_2 \rightarrow MCH_3OH \quad (8)$$

$$MCH_3OH \rightarrow M + CH_3OH \quad (9)$$

- Mechanism (b)

$$MOH + CO \rightarrow MOCOH \quad (10)$$

$$MOCOH + 2H_2 \rightarrow MOCH_3 + H_2O \quad (11)$$

$$MOCH_3 + H_2O \rightarrow MOH + CH_3OH \quad (12)$$

Mechanism (b) was supported by the experiments of Ueno et al. [55]. When they heated the methanol on the ZnO catalysts, the CH_3O and HCOO species were detected by the IR measurements. Since the CH_3O and HCOO species are not produced in the reaction mechanism (a), they suggested that the mechanism (b) is a reliable route for the methanol synthesis process. However, some problems have been pointed out for the mechanism (b). The excess number of oxygen atoms is essential for the synthesis of M–OCOH species, which only can be supplemented from ZnO or Al_2O_3 supports. However, when the CO^{18} gas was introduced to the catalysts, the formation of only $CH_3O^{18}H$ was detected and the formation of $CH_3O^{16}H$ was not observed [56]. It indicates that the excess oxygen is not supplemented from the ZnO or Al_2O_3 supports, which is against the mechanism (b). Other experiments also support the reaction mechanism (a) [57].

Hence, we employed both reaction mechanisms (a) and (b), and performed combinatorial computational chemistry based on the first-principles calculations to design new highly active catalysts for methanol synthesis [23,24]. Here, we summarized our recent results for the methanol synthesis reactions following the reaction mechanisms (a) and (b) in Sections 3.2 and 3.3, respectively. Several active sites were proposed and calculated for the methanol synthesis reactions on the Cu/ZnO catalysts. For example, French et al. calculated the methanol synthesis mechanism on ZnO($000\bar{1}$) surface by hybrid QM/MM method [7] and Martins et al. also employed ZnO surface as an active site [6]. However, Hu and Nakatsuji [1] and Morikawa et al. [2,3] mentioned that Cu/Zn site is most favorable for the methanol synthesis. Gomes and Gomes [4], Hu and Boyd [5], Kakumoto [8] and Kakumoto and Watanabe [9] employed Cu atom or cation as an active site for the methanol synthesis. On the other hand, experimentally Sugawa et al. investigated the activity of many metal/ZnO catalysts and found that the metal species strongly affect the catalytic activity for the methanol synthesis [58]. Hence in the present study we focused on the effect of the metal species on the methanol synthesis activity and the metal atom or metal cation is employed as an active site. Previously, Kakumoto [8] and Kakumoto and Watanabe [9] calculated the formation process of CH_3OH from CO_2 and H_2 on Cu and Cu^+ catalysts by using ab initio method. They employed only one metal atom or metal cation to represent the methanol synthesis catalysts. Hence, in the present study we followed their models and then the methanol synthesis catalysts are represented by one metal atom or one metal cation.

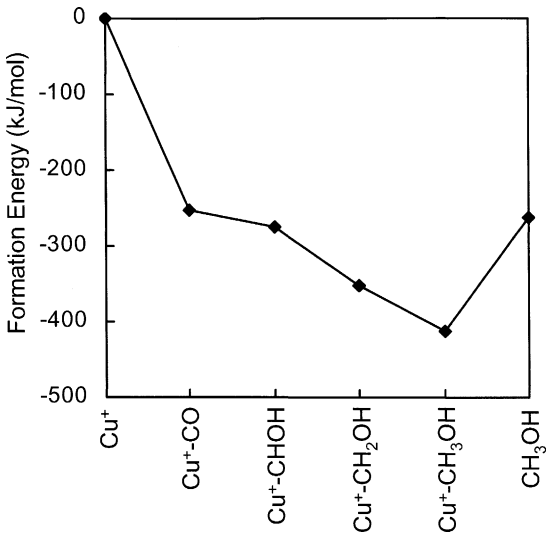

Fig. 1. Energy profile of the methanol synthesis process on Cu^+ catalyst, following the reaction mechanism (a) [23].

3.2. Design of new methanol synthesis catalysts based on mechanism (a) [23]

3.2.1. Energy profile of the intermediates for methanol synthesis process on Cu^+ cation

It has been already pointed out by many experiments that Cu^+ cation is an active site in the industrial Cu/ZnO/Al_2O_3 catalysts for the methanol synthesis [53,54]. Hence, first we employed the reaction mechanism (a) of the methanol synthesis process and investigated the formation energy of each intermediate on Cu^+ cation during the methanol synthesis process by using the first-principles calculations (Fig. 1). The formation of Cu^+–CH_3OH from $Cu^+ + CO + H_2$ through Cu^+–CO, Cu^+–CHOH, and Cu^+–CH_2OH takes place easily, since the energy curve is always decreased from $Cu^+ + CO + H_2$ to Cu^+–CH_3OH. This result indicates that Cu^+ cation is a favorable catalyst for the methanol synthesis, which is in good agreement with the previous experimental results [53,54].

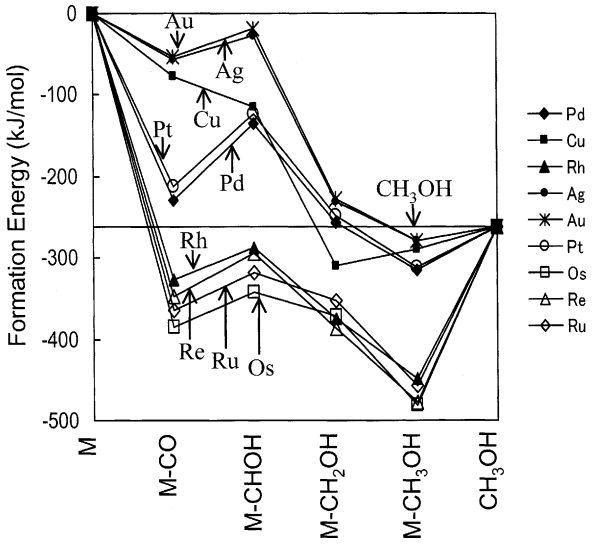

Fig. 2. Energy profile of the methanol synthesis process on various metal catalysts, following the reaction mechanism (a) (reprinted from Ref. [23] with permission from Elsevier).

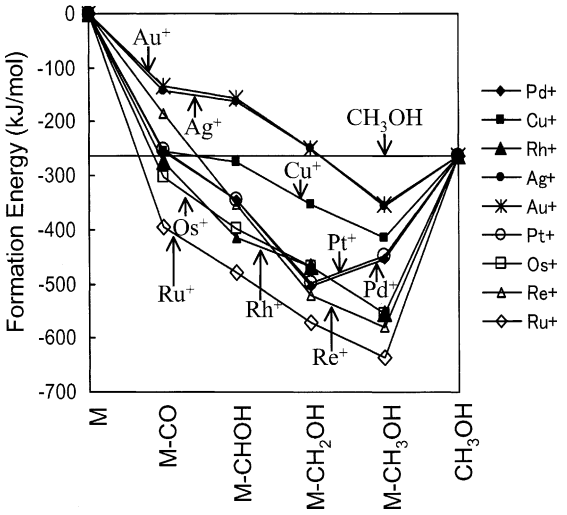

Fig. 3. Energy profile of the methanol synthesis process on various cationic metal catalysts, following the reaction mechanism (a) (reprinted from Ref. [23] with permission from Elsevier).

3.2.2. High-throughput screening of metal catalysts for methanol synthesis

We investigated the structures and energies of the intermediates during the methanol synthesis process on a lot of metal catalysts (Cu, Ru, Rh, Pd, Ag, Re, Os, Pt, and Au), following the reaction mechanism (a). Here, we selected 4d and 5d metals which have more than four electrons in their d orbitals since those metals have high activity in many catalytic reactions. Fig. 2 shows the energy profiles of various intermediates during the methanol synthesis process on the above catalysts. Center line in Fig. 2 shows the formation energy of methanol in the vapor phase from CO and H_2 (-262.84 kJ/mol). It indicates that this reaction is exothermic, which means that methanol synthesis reaction is energetically favorable.

This figure shows that the adsorption of CO molecule is exothermic on all the metal catalysts, which means that the adsorption of CO molecule is energetically favorable on all the metal catalysts. M–CHOH intermediate is unstable than M–CO intermediate on all metal catalysts except Cu catalyst. It indicates that the M–CHOH formation from M–CO is favorable only on the Cu catalyst. When we see the formation energy of M–CH_3OH intermediate, we noticed that these metal catalysts are divided into two groups. First group includes Cu, Pd, Ag, Pt, and Au has low formation energy of M–CH_3OH compared to the second group which includes Ru, Rh, Re, and Os. It indicates that the desorption of CH_3OH does not take place easily on the second group catalysts. Hence, Cu, Pd, Ag, Pt, and Au catalysts were found to be favorable for the easy desorption of CH_3OH from the catalysts.

However, compared to the energy profile on Cu^+ catalyst in Fig. 1, no favorable catalyst for the methanol synthesis was found from the energy profile on all the metal catalysts in Fig. 2. Only Cu catalyst gives the decrement energy from M–CO intermediate to M–CH_2OH intermediate, however it shows the increment energy from M–CH_2OH intermediate to M–CH_3OH intermediate on Cu catalyst. This energy profile on Cu catalyst is not favorable compared to Cu^+ catalyst in Fig. 1.

3.2.3. High-throughput screening of cationic metal catalysts for methanol synthesis

We cannot find good metal catalysts, which are more active than Cu^+ catalyst in Section 3.2.2. Hence, we also investigated the activities of the cationic metal catalysts, such as Cu^+, Ru^+, Rh^+, Pd^+, Ag^+, Re^+, Os^+, Pt^+, and Au^+, following the reaction mechanism (a). Fig. 3 shows the energy profiles of the intermediates during the methanol synthesis process on various cationic metal catalysts. This figure indicates that the formation of M–CH_3OH intermediate from $M + CO + H_2$ through M–CO, M–CHOH, and MCH_2OH takes place easily on all the cationic metal catalysts except Pt^+ and Pd^+, since their energy curves are always decreased. These results suggest that Au^+, Ag^+, Cu^+, Ru^+, Rh^+, Os^+, and Re^+ catalysts are favorable for the formation of M–CH_3OH intermediate from $M + CO + H_2$. These energy profiles are completely different form those on the metal catalysts in Fig. 2.

The formation energies of the M–CH_3OH are divided into two groups. The first group includes Cu^+, Pd^+, Ag^+, Pt^+, and Au^+ has small formation energy of M–CH_3OH, while the second group includes Ru^+, Rh^+, Re^+, and Os^+ has large formation energy. It indicates that the desorption of CH_3OH is very difficult on the second group catalysts. Hence, Cu^+, Pd^+, Ag^+, Pt^+, and Au^+ catalysts were found to be favorable for the desorption of CH_3OH, although the Pd^+ and Pt^+ catalysts are not favorable catalysts for the formation of M–CH_3OH from M–CH_2OH, which is

described before. Especially, the smaller formation energy of M–CH_3OH on the Ag^+ and Au^+ catalysts than the Cu^+ catalyst is noteworthy. Finally, we concluded that the Ag^+ and Au^+ catalysts are effective candidates for the methanol synthesis over the Cu^+ catalyst. Experimentally, Sugawa et al. found that Ag catalyst is active for the methanol synthesis from CO and H_2 [58], and Sakurai and Haruta shown that Au catalyst is also active for the same reaction [59]. These experimental results strongly support our combinatorial computational chemistry approach.

3.3. Design of new methanol synthesis catalysts based on mechanism (b) [24]

3.3.1. High-throughput screening of cationic metal catalysts for methanol synthesis

We also employed the reaction mechanism (b) of the methanol synthesis process, and investigated the formation energies of each intermediate on a lot of metal catalysts, such as Co, Cu, Ru, Rh, Pd, Ag, Re, Os, Ir, Pt, and Au, by using first-principles calculations. Following the reaction mechanism (b), we constructed the metal catalysts models such as CoOH, CuOH, RuOH, RhOH, PdOH, AgOH, ReOH, OsOH, IrOH, PtOH, and AuOH. Before the investigations on those catalysts, we investigated the catalytic activity of the cationic metal catalysts such as $(CoOH)^+$, $(CuOH)^+$, $(RuOH)^+$, $(RhOH)^+$, $(PdOH)^+$, $(AgOH)^+$, $(ReOH)^+$, $(OsOH)^+$, $(IrOH)^+$, $(PtOH)^+$, and $(AuOH)^+$, since cationic metal catalysts were found to be very active in Section 3.2.

Fig. 4 shows the energy profiles of various intermediates during the methanol synthesis process on cationic metal catalysts, following the reaction mechanism (b). Here, the center line also means the formation energy of methanol in the vapor phase from CO and H_2 (−262.84 kJ/mol). This figure indicates that the formation of M–OCOH intermediates from M–OH + CO takes place easily on all the cationic

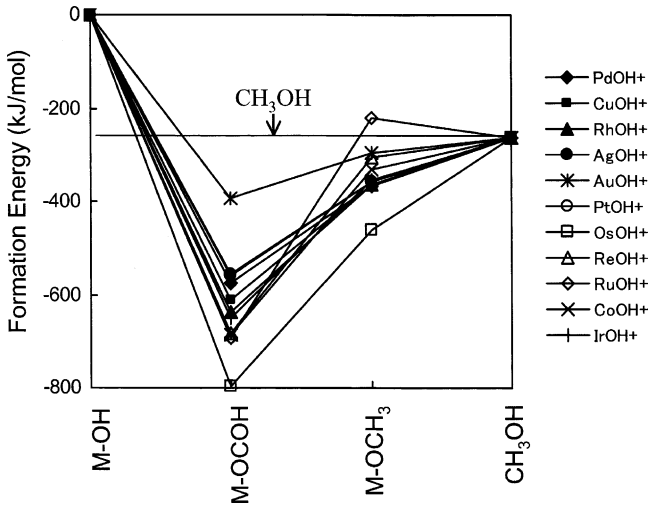

Fig. 4. Energy profile of the methanol synthesis process on various cationic metal catalysts, following the reaction mechanism (b) [24].

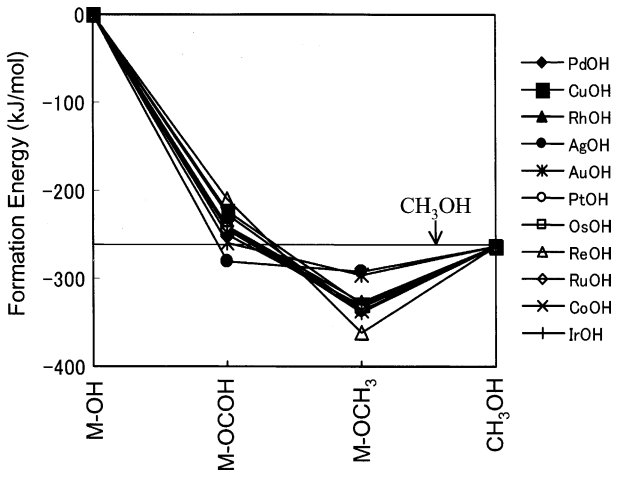

Fig. 5. Energy profile of the methanol synthesis process on various metal catalysts, following the reaction mechanism (b) [24].

metal catalysts, since the formation energies are decreased. However, it shows that the formation of M–OCH_3 intermediates from M–OCOH intermediates is significantly difficult on all the cationic metal catalysts since the formation energies are increased. These results indicate that all the cationic metal catalysts $(MOH)^+$ are not favorable for the formation of CH_3OH from CO and H_2, when we consider the reaction mechanism (b).

3.3.2. High-throughput screening of metal catalysts for methanol synthesis

We investigated the structures and energies of the intermediates during the methanol synthesis process on a lot of metal catalysts such as CoOH, CuOH, RuOH, RhOH, PdOH, AgOH, ReOH, OsOH, IrOH, PtOH, and AuOH, following the reaction mechanism (b). Fig. 5 shows the energy profiles of various intermediates during the methanol synthesis process on the above catalysts. This figure indicates that the formation of M–OCOH intermediate from M–OH + CO takes place easily on all the metal catalysts, since the formation energies are decreased. Furthermore, the formation of M–OCH_3 intermediate from M–OCOH intermediate takes place easily on all the metal catalysts, since the formation energies are decreased. These results indicate that all the metal catalysts MOH are favorable for the formation of M–OCH_3 intermediate from M–OCOH intermediate, when we consider the reaction mechanism (b). These energy profiles are completely different from those on the cationic metal catalysts shown in Fig. 4.

In order to design most favorable metal catalysts for the methanol synthesis reaction, we investigated the atomic bond population in M–OCOH intermediates (Fig. 6(a)). M–C atomic bond population of M–OCOH intermediates on various metal catalysts is shown in Table 1. The M–C atomic bond population on the Co, Cu, Pd, Ag, Ir, Pt, and Au catalysts is zero. These electronic states are favorable than that on the other catalysts because the M–C bond should be broken at the next step of the methanol synthesis

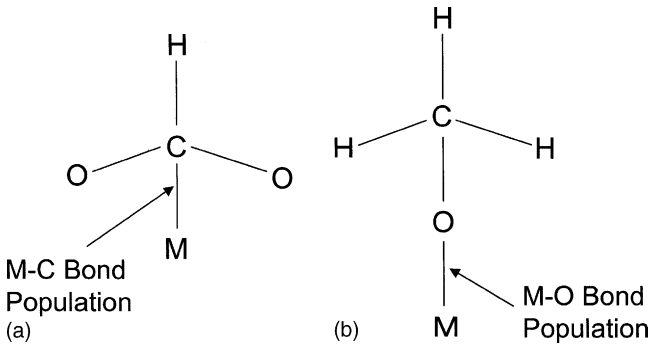

Fig. 6. Schematic structures of (a) M–OCOH and (b) M–OCH_3 intermediates (reprinted from Ref. [24] with permission from SPIE).

process. Moreover, we analyzed the M–O atomic bond population in M–OCH_3 intermediates (Fig. 6(b)). Table 1 also shows the M–O atomic bond population of M–OCH_3 intermediates on various metal catalysts. The M–O atomic bond population of M–OCH_3 intermediates on Cu, Pd, Ag, Ir, Pt, and Au catalysts is smaller than the other catalysts. These electronic features of M–OCH_3 intermediates on these metal catalysts progress the methanol synthesis reaction easily because the M–O bond should be broken and a new bond should be created at the next step of the methanol synthesis process. Hence, we concluded that the Cu, Pd, Ag, Ir, Pt and Au catalysts are effective candidates as methanol synthesis catalysts. Experimentally, Au, Ag, and Pd catalysts were found to be active for the methanol synthesis reaction [58–60], in addition to the Cu catalysts. These experimental results strongly support our combinatorial computational chemistry approach and we expected that the validity of other candidates would be confirmed experimentally in the near future.

In order to analyze the electronic states of the active catalysts, we investigated the charges on the metals in the M–OH and $(M–OH)^+$ states (Table 2). This table shows that the atomic charge on Cu atom in the CuOH is 0.40. It indicates that the cationic state of Cu has high activity, which is in agreement with the previous experimental results [53,54]. However, our calculation results show that the excessive cationic state of Cu is not favorable for the methanol synthesis reaction. Our calculation results show that $(CuOH)^+$ is not highly active in which Cu atom has 0.95 charge. The charges on the Pd, Ag, Ir, Pt and Au atoms in M–OH states are 0.33–0.48. We found that these slightly cationic states are favorable for the methanol synthesis reaction than full cationic states. The charges on the Pd, Ag, Ir, Pt and Au atoms in the $(M–OH)^+$ states are 0.95–1.05 and these excess cationic states are not favorable for the methanol synthesis. This proposed guidance of the favorable electronic states for the methanol synthesis catalysts may be very helpful for experimental researchers to design new methanol synthesis catalysts.

Table 1
M–C atomic bond population of M–OCOH intermediate and M–O atomic bond population of M–$OCOH_3$ intermediate (reprinted from Ref. [24] with permission from SPIE)

Metal (M)	M–C in M–OCOH	M–O in M–OCH_3
Co	0.00	1.10
Cu	0.00	0.97
Ru	0.15	1.01
Rh	0.17	0.99
Pd	0.00	0.78
Ag	0.00	0.81
Re	0.18	1.00
Os	0.14	1.02
Ir	0.00	0.97
Pt	0.00	0.75
Au	0.00	0.80

Table 2
Atomic charges on the metals in MOH and $(MOH)^+$ species (M = metal) (reprinted from Ref. [24] with permission from SPIE)

Metal (M)	MOH	$(MOH)^+$
Co	0.32	1.06
Cu	0.40	0.95
Ru	0.38	1.16
Rh	0.34	1.04
Pd	0.38	0.96
Ag	0.48	0.95
Re	0.36	1.19
Os	0.35	1.15
Ir	0.33	1.05
Pt	0.37	0.97
Au	0.47	0.95

4. Design of new Fischer–Tropsch catalysts [25–27]

4.1. Introduction

The interest in the Fischer–Tropsch (FT) synthesis, which is the conversion of a mixture of H_2 and CO to aliphatic hydrocarbons, has shown a large growth in the recent years [61]. The hydrocarbon synthesis is catalyzed by metal catalysts, such as Co, Fe, Ni, and Ru. Both Fe and Co are most commonly used in the industrial processes [62]. However, the use of FT catalysts is accompanied by their deactivation with several poisons such as sulfur-containing compounds. Moreover, the FT conversion is a polymerization reaction involving several intermediates and the control of product selectivity is also important topic. Therefore, the development of new catalysts with high activity, high selectivity, and high tolerance to poisons is strongly required for the new FT synthesis process. Hence, we have applied our combinatorial computational chemistry approach based on the first-principles calculations to the design of new Fe-based FT synthesis catalysts with high activity and high tolerance to sulfur [25–27]. In this review, we summarize our recent success in the design of new FT catalysts by using our combinatorial computational chemistry approach.

Table 3
Adsorption energies (E_{ads}), C–O distances (R_{C-O}), and charges (q_{CO}) of CO molecule adsorbed on various Fe_5M clusters (M = Fe, Si, Mn, Ge, Zr, and Mo) (reprinted from Ref. [25] with permission from SPIE)

System	E_{ads} (kJ/mol)	R_{C-O} (nm)	q_{CO}
Fe_6	−128.07	0.1152	−0.053
Fe_5Si	−95.44	0.1150	−0.040
Fe_5Mn	−138.91	0.1154	−0.067
Fe_5Ge	−97.49	0.1149	−0.040
Fe_5Zr	−133.85	0.1153	−0.053
Fe_5Mo	−154.43	0.1158	−0.064

4.2. CO adsorption on Fe/M catalysts (M = Fe, Si, Mn, Ge, Zr, and Mo)

In order to design effective additives for the Fe-based FT catalysts, we applied our combinatorial computational chemistry approach to the CO adsorption on Fe clusters. Fe(100) surface is imitated by an octahedral Fe_6 cluster which contains one atom in the first layer, four in the second layer, and one in the third layer. The effect of the additives on the molecular/cluster interaction is investigated using the Fe_5M (M = Fe, Si, Mn, Ge, Zr, and Mo) cluster model. In this model, one Fe atom from the second layer was substituted by the selected element. The interaction of substituted metals with sulfur would be much more stronger than that of Fe to protect the active sites of Fe catalysts against sulfur poisoning. Therefore, the elements such as Si, Ge, Zr, Mn, and Mo, which have a stronger interaction with S than that of Fe, were selected for this purpose [63].

The adsorption energies (E_{ads}), C–O distances, and charges of CO molecule adsorbed on the Fe_5M clusters are shown in Table 3. The negative charge on CO molecule, which is transferred from the metal atoms, indicates the activation of CO molecule by the metal cluster, since the lowest unoccupied orbital of CO molecule is anti-bonding. The C–O bond is significantly elongated compared to the C–O distance of 0.1128 nm in the vapor phase. The molecular orbital analysis shows that the π-back-donation mechanism of metal–CO bonding is responsible for the above electron transfer. Moreover, it was found that the Mn and Mo additives in the Fe cluster activate significantly CO molecule, since the C–O distance is elongated and the electron transfer is increased considerably on the Fe_5Mn and Fe_5Mo clusters, compared to those on the Fe_6 cluster. These electronic states changes by the incorporation of the Mn or Mo additive also lead to the increase in the adsorption energy of CO.

4.3. Design of new Fischer–Tropsch catalysts with high-tolerance to sulfur

In order to design new Fe-based FT catalysts with high-tolerance to sulfur, the difference in the adsorption energies of the CO and H_2S molecules on various Fe_5M (M = Fe, Si, Mn, Ge, Zr, and Mo) clusters were calculated (Fig. 7). Here, the negative value indicates that CO molecule

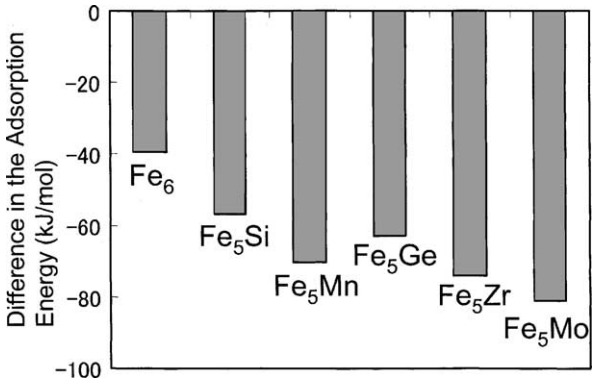

Fig. 7. Difference in the adsorption energies of CO and H_2S molecules on various Fe_5M clusters (M = Fe, Si, Mn, Ge, Zr and Mo) (reprinted from Ref. [25] with permission from SPIE).

is more strongly adsorbed on the metal cluster compared to H_2S molecule. Hence, the larger negative value, which means high-tolerance to H_2S poisoning, is favorable for FT catalysts. From this figure, Mn, Mo, and Zr additives were found to exhibit a high resistance to H_2S poisoning. As mentioned before, we predicted that Mn and Mo are effective to activate CO, which leads to high activity. Based on these results, we concluded that Mn and Mo are very effective additives in the Fe-based FT catalysts. Recently, Yamada and coworkers experimentally observed that the CO conversion does not decrease on the Fe/Mn catalyst in the presence of H_2S in syngas flow during a long time period [64]. This result strongly supports our prediction for the Fe/Mn system.

4.4. Catalytic reaction mechanism of CH_2 formation on Fe catalyst

FT synthesis is a multi-step reaction including reactant adsorption, chain initiation, chain growth, chain termination, product desorption, readsorption, and further reaction [62]. The formation of linear hydrocarbons involves a stepwise polymerization of CH_2 [65]. Hence, the formation of CH_2 is one of the important steps in the FT synthesis. Regarding the FT chain initiation, two different mechanisms were experimentally proposed. In the first pathway called carbide mechanism, CH_2 is formed by the breaking of the C–O bond and the following carbon hydrogenation. In the second pathway called hydroxy intermediate mechanism, H atom is adding first to adsorbed CO molecule and the formation of CHO, CHOH, and CH_2OH intermediates takes place. Experimentally, it is not clear which mechanism is feasible and realistic, yet.

Hence, we calculated the formation energies of various intermediates on the Fe_6 cluster, following two different mechanisms by using the first-principles calculations. The results are shown in Fig. 8. In the carbide mechanism, all the steps to the formation of $CH_2 + OH$ except CO dissociation is exothermic. On the other hand, in the hydroxy intermediate mechanism, the first two steps, CHO formation

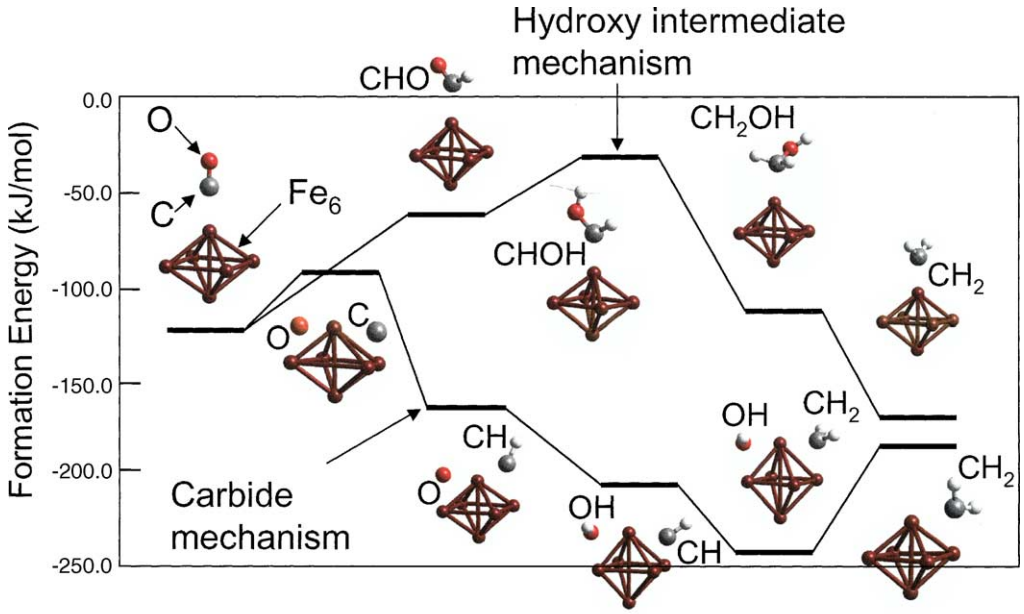

Fig. 8. Energy profile of CH_2 formation on Fe catalyst following the carbide mechanism and hydroxy intermediate mechanism (reprinted from Ref. [25] with permission from SPIE).

and CHOH formation, are significantly large endothermic reactions. These results indicate that the carbide mechanism is probable compared to the hydroxy intermediate mechanism, which is in agreement with many experiments [61,62]. Moreover, the chain initiation reaction was found to be significantly exothermic reaction, which also agrees well with the previous experiments [65].

4.5. Design of new Fischer–Tropsch catalysts with high activity

In order to design new FT catalysts with high activity, the reaction pathway of the chain initiation on various Fe/M catalysts (M = Si, Cr, Mn, Ge, Zr, and Mo) were investigated, following the carbide mechanism (Fig. 9). The energy profiles are significantly changed by the incorporation of metal additives, especially for the Fe_5Mo and Fe_5Zr clusters. The CO dissociation on the Fe_5Mo and Fe_5Zr clusters was found to be exothermic step, which is different from that on the Fe_6 cluster. Moreover, all the steps to the formation of $CH_2 + OH$ is exothermic on those catalysts. The formation process of $CH_2 + H_2O$ from $CH_2 + OH$ on both the Fe_5Mo and Fe_5Zr clusters is endothermic, and however the energy difference of $CH_2 + H_2O$ and $CH_2 + OH$ is very little on the Fe_5Mo cluster. Hence, these results suggest that the Fe_5Mo cluster is the most favorable catalyst for the CH_2 formation from CO and H_2.

As mentioned in Section 4.2 Fe_5Mo catalyst strongly activates CO molecule compared to that on other Fe/M catalysts, and as mentioned in Section 4.3 Fe_5Mo catalyst has high tolerance to sulfur. Hence, finally we concluded that the Mo is the most effective additive for the Fe-based FT

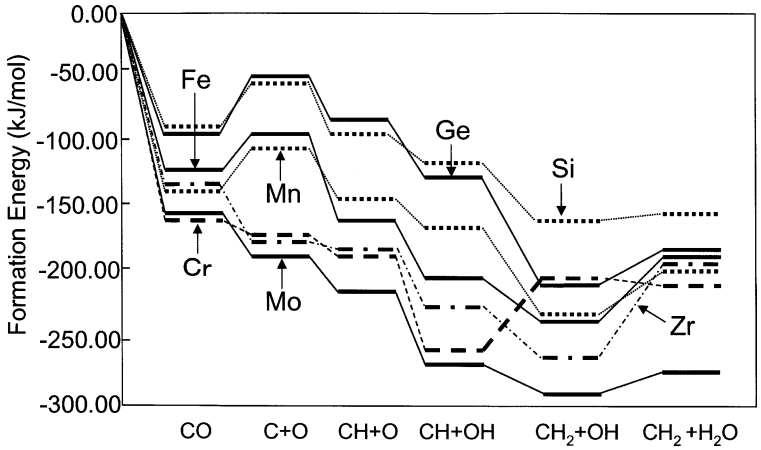

Fig. 9. Energy profile of CH_2 formation on various Fe_5M clusters (M = Fe, Si, Cr, Mn, Ge, Zr and Mo), following the carbide mechanism (reprinted from Ref. [25] with permission from SPIE).

catalyst to realize the high activity and high-tolerance to sulfur.

5. Design of new metal sulfide catalysts for the synthesis of high-quality transportation fuels [28]

5.1. Introduction

Recently, Koizumi et al. reported that a lot of metal sulfide catalysts have high activity for the CO hydrogenation process [66] and especially Rh sulfide has the highest activity and predominantly produces methanol [67]. Moreover, they found that the Rh sulfide catalyst is not deactivated by H_2S, while regular $Cu/ZnO/Al_2O_3$ methanol synthesis catalyst is easily deactivated by H_2S [67]. Moreover, they also reported that the products of the CO hydrogenation process are strongly depending on the metal species of the metal sulfide catalysts [68]. For example, Rh and Pd sulfides selectively produce methanol in the CO hydrogenation, while Re and Os sulfides predominantly produce hydrocarbons.

Hence, we applied our combinatorial computational chemistry to the metal sulfide catalysts and investigated the dependency of the metal species in the metal sulfide catalysts to the CO hydrogenation process and their products [28]. Moreover, the best metal sulfide catalyst with high selectivity for the methanol synthesis was successfully designed.

5.2. Selectivity of the CO hydrogenation on metal and metal sulfide catalysts

Our combinatorial computational chemistry approach was applied to the CO adsorption on various metal sulfide catalysts. We also calculated the CO adsorption on various metal catalysts for the comparison. To model the metal and metal sulfide catalysts, we employed diatomic molecules, M–M and M–S (M = metal, S = sulfur), respectively. Although it is better to employ the large catalyst model, we employed the simplest models to perform high-throughput screening for the present purpose. The elongation of the C–O distance may lead to the formation of hydrocarbons, while the shrinkage of the C–O distance may lead to the formation of methanol. Hence, we paid attention to the C–O distance of CO molecule adsorbed on various metal and metal sulfide catalysts. Table 4 shows the adsorption energy, charge, and C–O distance of CO molecule adsorbed on various catalysts. Here, the C–O distance of CO molecule in the vapor phase is 0.1128 nm. We found that the C–O distance of CO molecule adsorbed on all the metal and metal sulfide catalysts is elongated, compared to the C–O distance in the vapor phase. It indicates that CO molecule on all the catalysts is activated by the adsorption. Moreover, the C–O distance was found to be strongly depending on the metal species. The C–O distance is shortened on the Co, Mo, Ru, Rh, and Ir sulfide catalysts compared to that on their metal catalysts.

Table 4
Adsoprtion energy (E_{ads}), charge, and C–O distance of CO molecule adsorbed on various metal and metal sulfide catalysts (reprinted from Ref. [28] with permission from American Chemical Society)

Model	E_{ads} (kJ/mol)	CO charge	C–O distance (nm)
Co–Co	−192.54	−0.115	0.1155
Co–S	−122.05	−0.064 ↓	0.1148 ↓
Mo–Mo	−111.48	−0.292	0.1172
Mo–S	−171.93	−0.204 ↓	0.1165 ↓
Ru–Ru	−216.94	−0.366	0.1183
Ru–S	−236.14	−0.122 ↓	0.1157 ↓
Rh–Rh	−253.55	−0.324	0.1176
Rh–S	−216.97	−0.115 ↓	0.1150 ↓
Ir–Ir	−187.79	−0.675	0.1181
Ir–S	−241.83	−0.396 ↓	0.1158 ↓
Pd–Pd	−314.23	−0.342	0.1172
Pd–S	−205.77	0.189 ↓	0.1178 ↑
Re–Re	−101.73	−0.315	0.1158
Re–S	−180.00	−0.322 ↑	0.1168 ↑
Os–Os	−172.36	−0.447	0.1161
Os–S	−237.84	−0.390 ↓	0.1164 ↑

An arrow gives comparison with that on metal catalyst.

It indicates that these metal sulfide catalysts selectively produce methanol, which is in agreement with the experimental results by Koizumi et al. [66]. On the other hand, since the C–O distance is elongated on Re and Os sulfide catalysts compared to that on their metal catalysts, these metal sulfide catalysts are suggested to be very effective to produce hydrocarbons selectively, which is also in good agreement with the experimental results by Koizumi et al. [66].

5.3. Design of new metal sulfide catalysts for methanol synthesis

Moreover, we clarified that the Pd sulfide catalysts have the specific characteristics compared to the other metal sulfide catalysts. From the detailed analysis of the electronic states of the Pd sulfide catalyst, we suggested that the Pd sulfide has the highest selectivity of the methanol synthesis among all the metal sulfide catalysts, which is in agreement with the experimental result by Koizumi et al. [68]. CO molecule has the plus charge on the Pd sulfide catalysts, while CO molecule has the minus charge on the other metal and metal sulfide catalysts, as shown in Table 4. It was suggested that this difference is due to the different adsorption structure of CO molecule on the Pd sulfide and the other metal sulfide catalysts as shown in Fig. 10. CO molecule adsorbs on the on-top site of the metal species in the case of all the metal sulfide catalysts except the Pd sulfide. Hence, electrons transfer from metal species to CO molecule and then CO molecule gains minus charge on the most metal sulfide catalysts. Similarly, CO molecule surely adsorbs on the metal species in the case of all the metal cata-

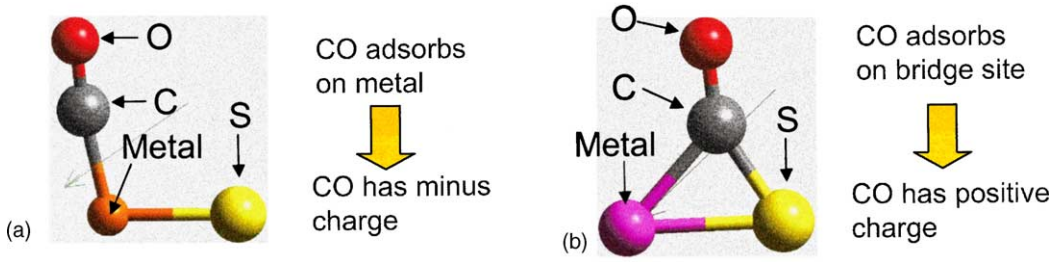

Fig. 10. Adsorption structures of CO molecule on the metal sulfide catalysts (reprinted from Ref. [28] with permission from American Chemical Society): (a) except Pd sulfide catalyst and (b) Pd sulfide catalyst.

lysts, and then electrons transfer from metal to CO molecule and the CO molecule gains minus charge. On the other hand, CO molecule adsorbs on the bridge-site of the Pd sulfide catalyst and contacts with both the Pd and sulfur atoms of the Pd sulfide. Hence, electrons transfer from CO molecule to the sulfur atom and the CO molecule gains plus charge.

Fig. 11 shows the molecular orbital of CO molecule. The LUMO and second LUMO of CO molecule are anti-bonding orbitals, and the electron has to be transferred to the above two orbitals of CO molecule from catalysts in order to dissociate CO molecule. However, CO molecule on the Pd sulfide catalyst has plus charge and then a large number of electrons have to be transferred to CO molecule from the catalysts after the adsorption in order to dissociate CO molecule. Hence, the dissociation of CO molecule is much difficult on the Pd sulfide catalyst compared to the other metal sulfide catalysts. This is the reason why we suggested that the Pd sulfide catalyst has the highest selectivity of the methanol. Moreover, we proposed that the metal sulfide catalysts, which realize the bridge-site adsorption of CO molecule on both the metal and sulfur atoms, have the high selectivity of the methanol. This proposed guidance to design the highly selective metal sulfide catalysts for methanol synthesis may be useful for the experimental researchers.

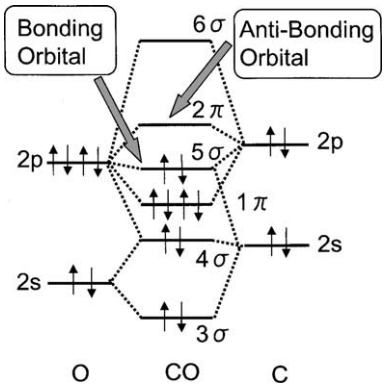

Fig. 11. Molecular orbitals of CO molecule (reprinted from Ref. [28] with permission from American Chemical Society).

6. Tight-binding quantum chemical molecular dynamics approach to methanol synthesis reaction dynamics [29]

6.1. Introduction

In Sections 3–5, we reviewed our combinatorial computational chemistry approach based on the first-principles calculations to the design of high-quality transportation fuels and introduced the success of the prediction of new catalysts. However, those calculations were applied to the static electronic states of catalysts at 0.0 K. In addition to the information on the static electronic states, the atomistic understanding of the catalytic reaction dynamics at reaction temperatures is very important for the catalysts research and design. First-principles molecular dynamics calculation can simulate the electronic states dynamics at reaction temperatures, however it requests huge computational costs and it can be applied to very small systems. Hence, the catalytic reaction dynamics on huge catalyst models including active metals, supports, and additives cannot be simulated by the first-principles molecular dynamics approaches.

Therefore, we have recently succeeded in the development of new tight-binding quantum chemical molecular dynamics software [29–36]. This software is based on our original tight-binding theory and realizes more than 5000 times acceleration compared to the regular first-principles molecular dynamics method. It means that our new software is very effective for the investigations of the catalytic reaction dynamics on huge catalyst models, compared to the first-principles molecular dynamics method. A lot of tight-binding approximations were already proposed by many researchers, and however those methods can calculate only the covalent systems, such as silicon and diamond [48–51]. Our new theory solved the above problem of the previous tight-binding theory, and hence it can be applied to all the materials including oxides, nitrides, sulfides, metals, and others. This is a main characteristic of our new tight-binding theory. The details of the theory is described in Section 2.3.

We have already applied the above software to various catalyst systems and have succeeded to clarify the atomistic catalytic reaction dynamics at reaction temperatures. Hence,

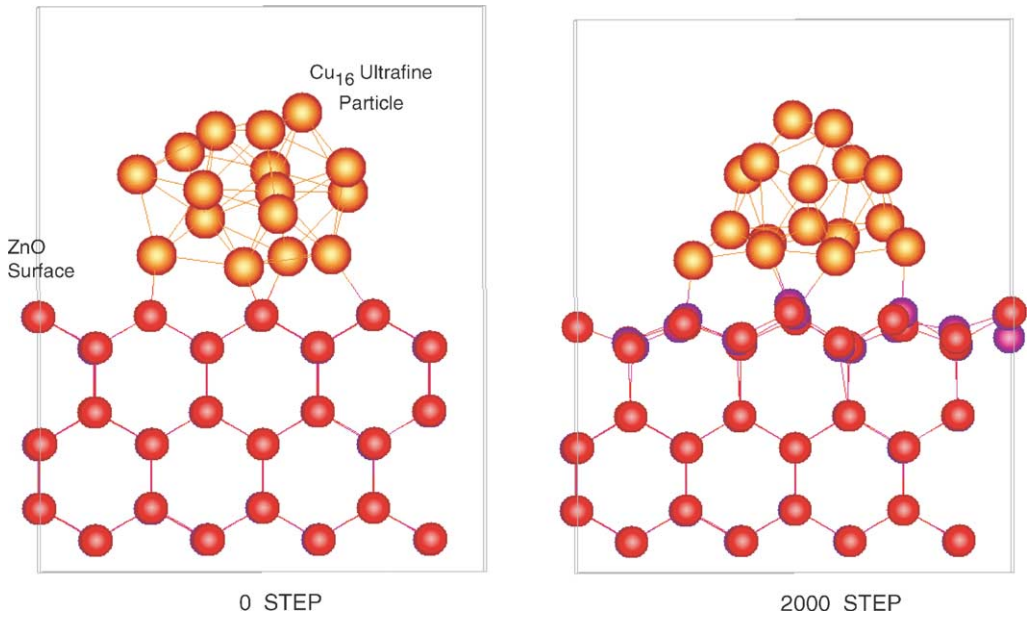

Fig. 12. Dynamic behavior of ultrafine Cu_{16} particle on the ZnO support calculated by our tight-binding quantum chemical molecular dynamics simulator (reprinted from Ref. [29] with permission from Elsevier).

here we summarized the recent applications of our new tight-binding quantum chemical molecular dynamics simulator to the Cu/ZnO methanol synthesis catalyst system and introduced our success in the clarification of the methanol synthesis reaction dynamics at reaction temperatures [29].

6.2. Quantum chemical molecular dynamics simulation of the ultrafine Cu particle on ZnO support

We constructed the Cu/ZnO catalyst model for the methanol synthesis reaction dynamics simulations. Ultrafine Cu_{16} particle was modeled and its structure was annealed by our tight-binding quantum chemical molecular dynamics simulator. Then, the ultrafine Cu_{16} particle was placed on the arbitrary position of the ZnO surface and the simulation was started in order to obtain the stable structure of the ultrafine Cu_{16} particle on the ZnO support. Here, ZnO($10\bar{1}0$) surface, which contains 96 atoms, was employed as the support. Fig. 12 shows the dynamics of the ultrafine Cu_{16} particle on the ZnO surface simulated by our simulator. Finally, the formation of the hemispherical, ultrafine Cu_{16} particle was observed on the ZnO support. It is interesting to see that the average charge of the Cu atoms on the ZnO support is +0.10, which indicates that the ZnO support strongly influences the electronic states of the ultrafine Cu_{16} particle. The above information cannot be obtained by the regular first-principles molecular dynamics simulator, since it requests large computational costs and cannot investigate large simulation model including both the ultrafine Cu particle and ZnO support. Hence, we confirmed that our tight-binding quantum chemical molecular dynamics simulator is very effective to calculate huge simulation models, which cannot be simulated by the regular first-principles molecular dynamics method.

6.3. Chemical reaction dynamics of methanol synthesis process calculated by tight-binding quantum chemical molecular dynamics simulator

The chemical reaction dynamics of the methanol synthesis process on the above huge Cu/ZnO catalyst model was simulated at reaction temperature of 500 K. Experimentally, the following reaction mechanism of the methanol synthesis process from CO_2 and H_2 on the Cu/ZnO catalyst was proposed [69]. First, CO_2 adsorbed on the Cu atom transforms to a formate intermediate. Second, formate intermediate transforms to formaldehyde intermediate and then transforms to metoxy intermediate. Finally, methanol is formed from metoxy intermediate and methanol is desorbed from the catalyst surface. Following the above reaction mechanism, we modeled the formate intermediate adsorbed on the Cu/ZnO catalyst. Moreover, H_2 molecule was placed at the arbitrary position close to the formate intermediate, and then quantum chemical molecular dynamics simulation was started. The simulation result is shown in Fig. 13. In this figure, the reaction site is magnified for well understanding, although the electronic states dynamics of all the atoms in Fig. 12 were calculated. After H_2 molecule approached to the reaction site, the dissociative adsorption of H_2 molecule was observed in Fig. 13. One of the dissociated H atoms formed a chemical bond with a C atom in the formate intermediate and another hydrogen atom formed a chemical bond with an O atom in the formate intermediate. Finally, we observed the formation of formaldehyde intermediate from the formate intermediate.

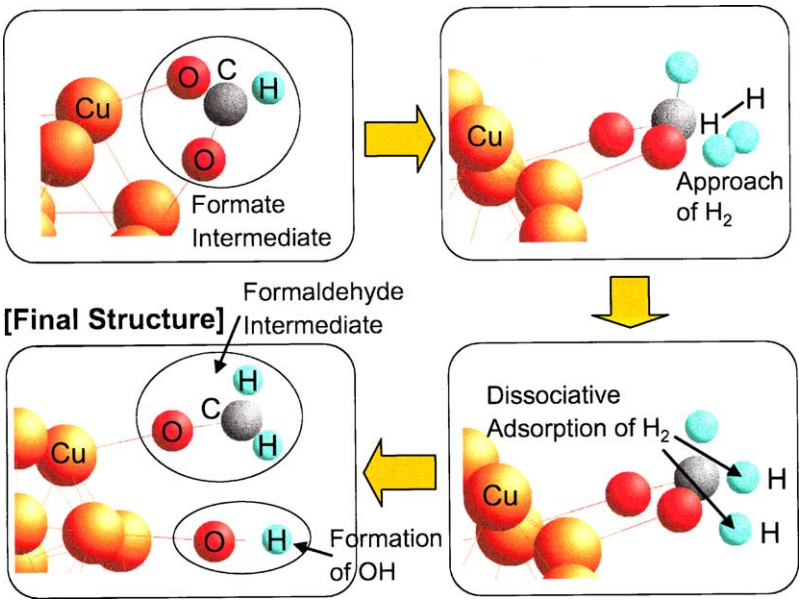

Fig. 13. Chemical reaction dynamics of the formate intermediate and H_2 molecule on the Cu/ZnO catalyst at 500 K (reprinted from Ref. [29] with permission from Elsevier).

The formation of formaldehyde intermediate from formate intermediate was suggested by the previous experiments [69].

Moreover, we also modeled the formaldehyde intermediate adsorbed on the Cu/ZnO catalyst. H_2 molecule was placed at the arbitrary position close to the formaldehyde intermediate, and then quantum chemical molecular dynamics simulation was started at reaction temperature of 500 K. The simulation result is shown in Fig. 14. In this figure the reaction site is magnified for good understanding, although the electronic states dynamics of all the atoms in Fig. 12 were calculated. After the H_2 molecule approached to the reaction site, the dissociative adsorption of the H_2 molecule was observed in Fig. 14. One of the dissociated H atoms formed a chemical bond with a C atom in the formaldehyde intermediate and another H atom formed a chemical bond with an O atom in the formaldehyde intermediate. Finally, we observed the formation of methanol through metoxy intermediate and then the desorption of the methanol was successfully simulated. The formation of methanol from

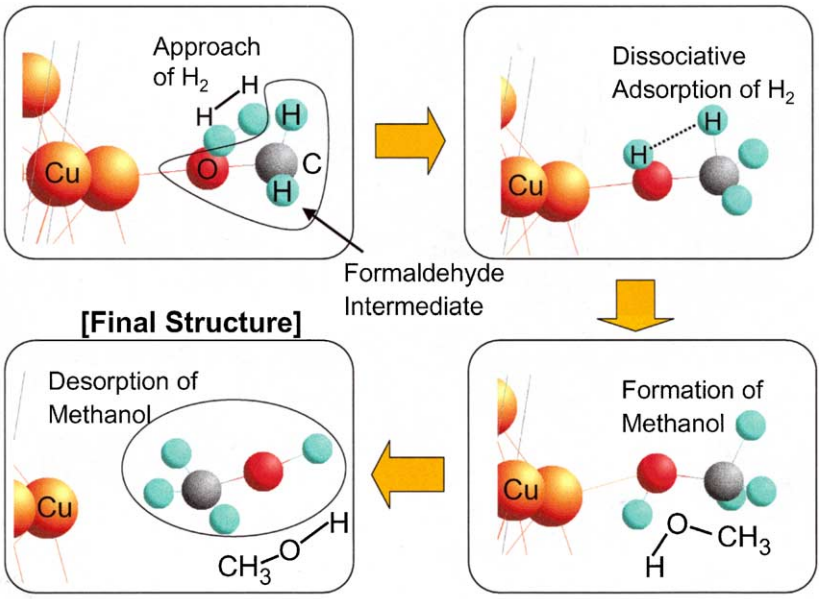

Fig. 14. Chemical reaction dynamics of the formaldehyde intermediate and H_2 molecule on the Cu/ZnO catalyst at 500 K (reprinted from Ref. [29] with permission from Elsevier).

formaldehyde intermediate through metoxy intermediate was also suggested by the previous experiments [69].

Our tight-binding quantum chemical molecular dynamics calculations well reproduced the previous experiments, although the regular first-principles molecular dynamics method cannot simulate the chemical reaction dynamics on huge catalyst models and clarify the effect of supports and additives. Moreover, our tight-binding quantum chemical molecular dynamics method can clarify more detailed information such as the changes in the charge, bond population, electron transfer, and so on during the catalytic reactions. Such information will significantly contribute to the understanding of the catalytic reaction dynamics and the elucidation of the reason why the Cu/ZnO catalyst has high activity. Finally, we confirmed that our chemical reaction dynamics simulator based on our original tight-binding quantum chemical molecular dynamics method is very effective to simulate the catalytic reaction dynamics and to predict the final products from the reactants. Moreover, the combination of tight-binding quantum chemical molecular dynamics method and combinatorial computational chemistry approach will be very effective tool for the high-throughput screening of the catalysts. Hence, in the near future we would like to perform combinatorial computational chemistry approach based on the tight-binding quantum chemical molecular dynamics method for the design of new methanol synthesis catalysts from CO_2 and H_2.

7. Conclusions

In the present paper, first we reviewed our combinatorial computational chemistry approach to the design of new catalysts for methanol synthesis and Fischer–Tropsch synthesis by using grid-computing technology. As described in the present paper, many calculation results were in good agreement with the previous experiments and some new catalysts were successfully predicted by our combinatorial computational chemistry approach. Hence, we concluded that our combinatorial computational chemistry is very accurate and effective approach for the design of new catalysts. We expect that our proposed catalysts in the present paper will be experimentally confirmed and industrialized. Moreover, in the near future our combinatorial computational chemistry will be applied to the transition state search and the estimation of the activation barrier for many catalytic reactions. This approach will change our combinatorial computational chemistry technique to more powerful tool for the theoretical catalyst design.

We also summarized the recent applications of our tight-binding quantum chemical molecular dynamics method to the clarification of the catalytic reaction dynamics at reaction temperatures and confirmed that this new software is very effective, powerful, and practical to simulate the catalytic reaction dynamics on huge catalyst models including active metals, supports, and additives, compared to the regular first-principles molecular dynamics method. Application of our new simulator is now expanding to the wide-range area of the catalysts fields. We are expecting that our tight-binding quantum chemical molecular dynamics method significantly increases the impacts and effectiveness of computational chemistry to catalysts development as well as in the near future a lot of catalysts designed by the above new simulator will be commercialized and industrialized.

Acknowledgements

This work was supported by Research for the Future Program of Japan Society for the Promotion of Science under the Project “Synthesis of Ecological High Quality Transportation Fuels” (JSPS-RFTF98P01001).

References

[1] Z.-M. Hu, H. Nakatsuji, Chem. Phys. Lett. 313 (1999) 14.
[2] Y. Morikawa, K. Iwata, J. Nakamura, T. Fujitani, K. Terakura, Chem. Phys. Lett. 304 (1999) 91.
[3] Y. Morikawa, K. Iwata, K. Terakura, Appl. Surf. Sci. 169/170 (2001) 11.
[4] J.R.B. Gomes, J.A.N.F. Gomes, Surf. Sci. 432 (1999) 279.
[5] Z. Hu, R.J. Boyd, J. Chem. Phys. 112 (2000) 9562.
[6] J.B.L. Martins, C.A. Taft, S.K. Lie, E. Longo, J. Mol. Struct. (Theochem.) 528 (2000) 161.
[7] S.A. French, A.A. Sokol, S.T. Bromley, C.R.A. Catlow, S.C. Rogers, F. King, P. Sherwood, Angew. Chem. 113 (2001) 4569.
[8] T. Kakumoto, Energy Convers. Manage. 36 (1995) 661.
[9] T. Kakumoto, T. Watanabe, Catal. Today 36 (1997) 39.
[10] Y. Matsumoto, M. Murakami, Z. Jin, A. Ohtomo, M. Lippmaa, M. Kawasaki, H. Koinuma, Jpn. J. Appl. Phys. 38 (1999) L603.
[11] Y. Matsumoto, M. Murakami, T. Shono, T. Hasegawa, T. Fukumura, M. Kawasaki, P. Ahmet, T. Chikyow, S. Koshihara, H. Koinuma, Science 291 (2001) 854.
[12] R.B. van Dover, L.F. Schneemeyer, R.M. Fleming, Nature 392 (1998) 162.
[13] E. Danielson, J.H. Golden, E.W. McFarland, C.M. Reaves, W.H. Weinberg, X.D. Wu, Nature 389 (1997) 944.
[14] G. Briceno, H. Chang, X. Sun, P.G. Schultz, X.D. Xiang, Science 270 (1995) 273.
[15] S.M. Senkan, Nature 394 (1998) 350.
[16] D.E. Akporiaye, I.M. Dahl, A. Karlsson, R. Wendelbo, Angew. Chem. Int. Ed. Engl. 37 (1998) 609.
[17] S. Senkan, K. Krantz, S. Ozturk, V. Zengin, I. Onal, Angew. Chem. Int. Ed. Engl. 38 (1999) 2794.
[18] K. Yajima, Y. Ueda, H. Tsuruya, T. Kanougi, Y. Oumi, S.S.C. Ammal, S. Takami, M. Kubo, A. Miyamoto, Appl. Catal. A 194/195 (2000) 183.
[19] K. Yajima, S. Sakahara, Y. Ueda, R. Belosludov, S. Takami, M. Kubo, A. Miyamoto, Proc. SPIE 3941 (2000) 62.
[20] K. Yajima, Y. Ueda, H. Tsuruya, T. Kanougi, Y. Oumi, S.S.C. Ammal, S. Takami, M. Kubo, A. Miyamoto, Stud. Surf. Sci. Catal. 130 (2000) 401.
[21] R. Belosludov, S.S.C. Ammal, Y. Inaba, Y. Oumi, S. Takami, M. Kubo, A. Miyamoto, M. Kawasaki, M. Yoshimoto, H. Koinuma, Proc. SPIE 3941 (2000) 2.
[22] K. Suzuki, Y. Kuroiwa, S. Takami, M. Kubo, A. Miyamoto, Appl. Surf. Sci. 189 (2002) 313.

[23] S. Sakahara, K. Yajima, R. Belosludov, S. Takami, M. Kubo, A. Miyamoto, Appl. Surf. Sci. 189 (2002) 253.
[24] S. Sakahara, K. Yajima, R. Belosludov, S. Takami, M. Kubo, A. Miyamoto, Proc. SPIE 4281 (2001) 97.
[25] R.V. Belosludov, T. Kubota, S. Sakahara, K. Yajima, S. Takami, M. Kubo, A. Miyamoto, Proc. SPIE 4281 (2001) 87.
[26] R.V. Belosludov, S. Takami, M. Kubo, A. Miyamoto, Y. Kawazoe, Mater. Trans. 40 (2001) 2180.
[27] R.V. Belosludov, S. Sakahara, K. Yajima, S. Takami, M. Kubo, A. Miyamoto, Appl. Surf. Sci. 189 (2002) 245.
[28] M. Kubo, T. Kubota, C. Jung, K. Seki, S. Takami, N. Koizumi, K. Omata, M. Yamada, A. Miyamoto, Energy and Fuels 17 (2003) 853.
[29] M. Kubo, M. Ando, S. Sakahara, C. Jung, K. Seki, T. Kusagaya, A. Endou, S. Takami, A. Imamura, A. Miyamoto, Appl. Surf. Sci. 223 (2004) 188.
[30] M. Elanany, P. Selvam, T. Yokosuka, S. Takami, M. Kubo, A. Imamura, A. Miyamoto, J. Phys. Chem. B 107 (2003) 1518.
[31] Y. Luo, P. Selvam, Y. Ito, S. Takami, M. Kubo, A. Imamura, A. Miyamoto, Organometallics 22 (2003) 2181.
[32] T. Yokosuka, K. Sasata, H. Kurokawa, S. Takami, M. Kubo, A. Imamura, A. Miyamoto, Jpn. J. Appl. Phys. 42 (2003) 1897.
[33] K. Sasata, T. Yokosuka, H. Kurokawa, S. Takami, M. Kubo, A. Imamura, T. Shinmura, M. Kanoh, P. Selvam, A. Miyamoto, Jpn. J. Appl. Phys. 42 (2003) 1859.
[34] K. Suzuki, Y. Kuroiwa, S. Takami, M. Kubo, A. Miyamoto, A. Imamura, Solid State Ionics 152/153 (2002) 273.
[35] H. Takaba, A. Endou, A. Yamada, M. Kubo, K. Teraishi, K.G. Nakamura, K. Ishioka, M. Kitajima, A. Miyamoto, Jpn. J. Appl. Phys. 39 (2000) 2744.
[36] A. Yamada, A. Endou, H. Takaba, K. Teraishi, S.S.C. Ammal, M. Kubo, K.G. Nakamura, M. Kitajima, A. Miyamoto, Jpn. J. Appl. Phys. 38 (1999) 2434.
[37] P. Hohenberg, W. Kohn, Phys. Rev. B 136 (1964) 865.
[38] W. Kohn, L. Sham, Phys. Rev. A 140 (1965) 1133.
[39] B. Delley, J. Chem. Phys. 92 (1990) 508.
[40] B. Delley, J. Chem. Phys. 94 (1991) 7245.
[41] E.J. Baerends, D.E. Ellis, D.P. Ros, Chem. Phys. 2 (1973) 41.
[42] E.J. Baerends, D.P. Ros, Chem. Phys. 2 (1973) 51.
[43] P.M. Boerringt, G. te Velde, E.J. Baerends, Int. J. Quant. Chem. 33 (1988) 87.
[44] G. te Velde, F.M. Bickelhaupt, E.J. Baerends, C. Fonseca Guerra, S.J.A. van Gisbergen, J.G. Snijders, T. Ziegler, J. Comp. Chem. 22 (2001) 931.
[45] S.H. Vosko, L. Wilk, M. Nusair, Can. J. Phys. 58 (1980) 1200.
[46] A.D. Becke, Phys. Rev. A 38 (1988) 3098.
[47] J.P. Perdew, Y. Wang, Phys. Rev. B 45 (1992) 13244.
[48] K. Lassonen, R.M. Nieminen, J. Phys. Condens. Matter 2 (1990) 1509.
[49] B.J. Min, Y.H. Lee, C.Z. Wang, C.T. Chan, K.M. Ho, Phys. Rev. B 46 (1992) 9677.
[50] S. Goedecker, L. Colombo, Phys. Rev. Lett. 73 (1994) 122.
[51] M. Menon, K.R. Subbaswamy, Phys. Rev. B 51 (1995) 17952.
[52] R. Miura, H. Yamano, R. Yamauchi, M. Katagiri, M. Kubo, R. Vetrivel, A. Miyamoto, Catal. Today 23 (1995) 409.
[53] R.G. Herman, J. Catal. 56 (1979) 407.
[54] S. Mehta, G.W. Simmons, K. Klier, R.G. Herman, J. Catal. 57 (1979) 339.
[55] A. Ueno, T. Onishi, K. Tamaru, Trans. Faraday Soc. 67 (1971) 3585.
[56] F. Boccuzzi, E. Borello, A. Zecchiina, A. Bossi, M. Camia, J. Catal. 51 (1964) 150.
[57] J.C. Tracy, J. Chem. Phys. 56 (1972) 2748.
[58] S. Sugawa, K. Sayama, K. Okabe, H. Arakawa, Energy Convers. Manage. 36 (1995) 665.
[59] H. Sakurai, M. Haruta, Appl. Catal. A 127 (1995) 93.
[60] S. Fujita, M. Usui, T. Hanada, N. Takezawa, React. Kinet. Catal. Lett. 56 (1995) 15.
[61] H. Schultz, Appl. Catal. A 186 (1999) 3.
[62] G.P. van der Laan, A.A.C.M. Beenackers, Catal. Rev.-Sci. Eng. 41 (1999) 255.
[63] D.R. Lide (Ed.), CRC Handbook of Chemistry and Physics, 79th ed., CRC Press, Boca Raton, FL, 1998.
[64] M. Jiang, N. Koizumi, M. Yamada, J. Phys. Chem. B 104 (2000) 7636.
[65] P.M. Maitlis, R. Quyoum, H.C. Long, M.L. Turner, Appl. Catal. A 186 (1999) 363.
[66] N. Koizumi, T. Furukawa, A. Miyazawa, T. Ozaki, Y. Takahashi, M. Yamada, in: Proceedings of the International Symposium on Synthesis of Ecological High Quality Transportation Fuels, 2000, p. 53.
[67] M. Yamada, N. Koizumi, A. Miyazawa, T. Furukawa, Catal. Lett. 78 (2002) 195.
[68] N. Koizumi, A. Miyazawa, T. Furukawa, M. Yamada, Chem. Lett. (2001) 1282.
[69] S. Fujita, Y. Kanamori, A.M. Satriyo, N. Takezawa, Catal. Today 45 (1998) 241.